CHAPTER-9

EFFECT OF LASER BEAM WIDTH PARAMETER ON ELECTRON ACCELERATION IN MAGNETIZED PLASMA

9.1 INTRODUCTION

Tajima and Dawson proposed the concept of laser-driven accelerators focused on plasma about three decades ago [1]. Accordingly the electron trapped in laser field gets accelerated to high energy due to laser. The characteristic variation in laser beam parameters and laser profiles has been investigated theoretically and several experimental models have been presented for high energy gain by electrons [12, 13, 22, 57, 60, 69]. Polarization plays a vital role in electron acceleration during interaction of laser beams with plasma. Linearly, circularly, and radially polarized (RP) laser beams has extensively studied for higher energy gain by electron during laser-electron interaction. Malka *et al.* [13] investigated experimentally the acceleration of electrons in vacuum to MeV energies by a high-intensity sub-picosecond linearly polarized (LP) laser pulse ($10^{19} W/cm^2$, $300 fs$). Tsakiris *et al.* [22] have developed an analytical model based on direct laser acceleration for frozen refractive indexed plasma with the interactive propagation of relativistic laser pulse. The electrons at leading of the Gaussian laser pulse are accelerated due to the application of ponderomotive force of the laser pulse. Hu and Starace [57] observed about 100MeV of energy by rest electron with a LP laser pulse of peak intensity ($2\times10^{22} W/cm^2$, $1.054 \mu m$) and beam waist of $10 \mu m$. In an experiment with laser-driven plasma accelerator, the acceleration gradient of about $10 GeV/m$ was reported with emergence of a mono-energetic and low divergence electron beams in $100 MeV - 1 GeV$ range [69]. Fortin *et al.* [91] studied the dependence of energy gained by electron on the power of laser, laser beam waist, and duration of pulse for electron acceleration. Gaussian profile of laser pulse proves its suitability for electron acceleration because of its ability to generate high energy, narrow divergence electron beams of constricts energy spread [66]. The fields of lowest order RP Gaussian laser beam were employed to accelerate electrons to energy range of GeV [61]. The Gaussian beam fields are determined by

laser beam frequency ω, radius of beam waist r_0 at the focus, and Rayleigh length $Z_R = kr_0^2/2$. Singh *et al*. [83] demonstrated the enhancement in electron energy by using a CP Gaussian laser pulse during laser-electron interaction. It is the axial symmetry of the CP pulse which attributes the energy enhancement of electrons. The chirped pulse amplification (CPA) with characteristics variations of laser frequency ensures the availability of ultra-intense ($\approx 10^{22} W/cm^2$) and ultra-short laser for electron acceleration [117, 121]. Afhami and Eslami analysed the impact of different chirped Gaussian laser pulse interaction with plasma [117]. Accordingly an ultra-short laser pulse interactively passing through plasma can stimulate a nonlinear plasma wake field. Such field can accelerate charged particles up to energies of the order of GeV within compact dimensions as compared to conventional accelerator devices. Enhancement in electron acceleration appears, if a suitable and static magnetic field is applied externally [58, 126]. The externally applied magnetic field enhances $\vec{v} \times \vec{B}$ force due to which the electron accelerates efficiently in the direction parallel to the propagation of the laser pulse. Additional acceleration by magnetic field resonance [58] at very high intensity laser interaction was proposed with spontaneous magnetic field of $100MG$. About 70% higher electron energy was observed with an externally applied axial magnetic field than that in the absence of static magnetic field with a RP laser pulse [126]. Feng *et al*. [49] studied the vacuum acceleration of electron with a Gaussian laser pulse. They proposed that the evolution of the laser beam waist cannot be ignored when the electron drifting distance is of the order of Rayleigh length. Thus, the electron can efficiently be accelerated and drawn out by the longitudinal ponderomotive force due to Gaussian laser beam. The electron energy gain of few MeV was realized with a Gaussian laser beam of intensity above $10^{19} W/cm^2$. Most of the previous studies have assumed a continuous laser beam with a fixed waist size for electron acceleration [8, 16, 36, 72, 110]. This presented a challenge that the acceleration of electrons is possible only at the front side of the laser pulse. Due to which the electrons are unable to face the peak intensity of the pulse. Hence do not enter in the high electric fields of petawatt (PW) laser.

In this chapter we present the influence of beam width parameter on electron acceleration by using a relativistic 3-D single particle code with a CP Gaussian laser pulse in magnetized plasma. We investigate the effect of laser beam width parameter on electron acceleration with variation of laser intensity. High energy gain is realized in the presence of high intensity laser pulse. We compare the acceleration distance in term of Rayleigh length for different values of laser beam spot size. The greater count of Rayleigh length in terms of propagation distance is observed for a smaller beam spot size and vice versa. The electron gain high energy with small beam width parameter due to strong laser field and loss energy with large beam width due to weak field with large propagation distance. The externally applied axial magnetic field supports the retaining of high energy by electron for large distance. We obtain a very high acceleration gradient with small ejection of electrons due to axial magnetic field in plasma. This content of rest part of this paper is arranged as follows. Section 9.2 and 9.3 explains the electromagnetic fields and electron dynamics required to study electron acceleration. Outcomes are discussed in section 9.4. Finally, conclusion is drawn in the section 9.5.

9.2 FIELD DISTRIBUTION AND BEAM WIDTH PARAMETER FOR A GAUSSIAN BEAM

The transverse electric field components for a CP Gaussian laser beam propagating in the z-direction, under paraxial approximation can be written as [63, 22]:

$$E_x(r,z,t)=\frac{E_0}{f(z)}\exp(i\phi)\exp\left(-\frac{(t-\frac{z-z_L}{c})^2}{\tau^2}-\frac{r^2}{r_0^2 f^2}\right), \tag{9.1}$$

$$E_y(r,z,t)=\frac{E_0}{f(z)}\exp\left[i\left(\phi+\frac{\pi}{2}\right)\right]\exp\left(-\frac{(t-\frac{z-z_L}{c})^2}{\tau^2}-\frac{r^2}{r_0^2 f^2}\right), \tag{9.2}$$

where E_0 is the amplitude of electric field, ϕ is the Gaussian beam phase, τ is the pulse duration, z_L is the initial position of the pulse peak, $r^2 = x^2 + y^2$, r_0 is the minimum laser spot size, and c is the velocity of light.

Other Gaussian beam parameters are defined as [8]:

$$f(z) = \sqrt{1+\xi^2}\,, \tag{9.3}$$

where $f(z)$ is the laser beam width parameter, $\xi = z/Z_R$ is the normalized propagation distance, $Z_R = kr_0^2/2$ is the Rayleigh length, k is the laser wave number, $\phi = \omega_0 t - kz + \tan^{-1}(\xi) - zr^2/(Z_R r_0^2 f^2) + \phi_0$, ω_0 is the laser frequency, $\tan^{-1}(\xi)$ is the Guoy phase, and ϕ_0 is the initial phase.

The axial magnetic field is expressed as [80]:

$$\vec{B} = B_0 \hat{z}\,. \tag{9.4}$$

To express the laser fields correctly, in addition to transverse electric components, axial guide, the longitudinal electric component and magnetic components are express by paraxial approximation as:

$$E_z(r,z,t) = -\left(\frac{i}{k}\right)\left(\frac{\partial E_x}{\partial x} + \frac{\partial E_y}{\partial y}\right), \tag{9.5}$$

$$\vec{B}(r,z,t) = -\left(\frac{i}{\omega}\right)\left(\vec{\nabla}\times\vec{E}\right). \tag{9.6}$$

Figure 9.1 represents a scheme of acceleration of electron by a CP Gaussian laser pulse in plasma under the influence of externally applied axial magnetic field.

We have considered a plasma with a density about $10^{23} m^{-3}$, and a laser pulse of the wavelength $\lambda = 1.054 \mu m$. Therefore the plasma frequency and the frequency of laser pulse are $\omega_p = 1.8\times10^{13} rad/s$ and $\omega_0 = 1.8\times10^{15} rad/s$ respectively. Hence, $\omega_p^2/\omega_0^2 \approx 10^{-4}$. It has been experimentally proved that at this plasma density (with pressure $\approx 1 Torr$), plasma effects such as wake-fields, plasma instabilities, and modification of amplitude can be neglected [32].

9.3 ELECTRON DYNAMICS AND RELATIVISTIC ANALYSIS

The momentum and energy of electron are expressed in terms of following equations:

$$\frac{dp_x}{dt} = -eE_x + e\beta_z B_y - e\beta_y (B_z + B_0), \tag{9.7}$$

$$\frac{dp_y}{dt} = -eE_y - e\beta_z B_x + e\beta_x (B_z + B_0), \tag{9.8}$$

$$\frac{dp_z}{dt} = -eE_z - e(\beta_x B_y - \beta_y B_x), \tag{9.9}$$

$$\frac{d\gamma}{dt} = -e(\beta_x E_x + \beta_y E_y + \beta_z E_z), \tag{9.10}$$

where (p_x, p_y, p_z) are the (x, y, z) coordinates of the momentum $\vec{p} = \gamma m_0 \vec{v}$;

($\beta_x, \beta_y, \beta_z$) are the (x, y, z) coordinates of the normalized velocity $\vec{\beta} = \vec{v}/c$; $\gamma^2 = 1 + (p_x^2 + p_y^2 + p_z^2)/(m_0 c)^2$ is the Lorentz factor, $-e$ and m_0 are the charge and rest mass of electron respectively.

The dimensionless variables are expressed as follow:

$$a_0 \to \frac{eE_0}{m_0 \omega_0 c},\ \tau' \to \omega_0 \tau,\ r_0' \to \frac{\omega_0 r_0}{c},\ z_L' \to \frac{\omega_0 z_L}{c},\ x' \to \frac{\omega_0 x}{c},\ y' \to \frac{\omega_0 y}{c},\ z' \to \frac{\omega_0 z}{c},$$

$$\beta_x \to \frac{v_x}{c},\ \beta_y \to \frac{v_y}{c},\ \beta_z \to \frac{v_z}{c},\ t' \to \omega_0 t,\ p_0' \to \frac{p_0}{m_0 c},\ p_x' \to \frac{p_x}{m_0 c},\ p_y' \to \frac{p_y}{m_0 c},$$

$$p_z' \to \frac{p_z}{m_0 c},\ k' \to \frac{ck}{\omega_0}, \text{ and } b_0 \to \frac{eB_0}{m_0 \omega_0 c}.$$

Equations (9.7)-(9.10) are the coupled differential equations. These equations have been solved numerically with a computer simulation code for electron energy.

9.4 RESULTS AND DISCUSSION

We have chosen the following dimensionless parameters for numerical analysis: $a_0 = 5$ (represents laser intensity $I \sim 6.92 \times 10^{19}\ W/cm^2$), $a_0 = 25$ (represents laser intensity $I \sim 8.5 \times 10^{20}\ W/cm^2$), $a_0 = 50$ (represents laser intensity $I \sim 6.8 \times 10^{21}\ W/cm^2$); $r_0' = 150$ (represents laser spot size $r_0 \sim 25\mu m$), $r_0' = 300$ (represents laser spot size $r_0 \sim 50\mu m$), $r_0' = 450$ (represents laser spot size $r_0 \sim 75\mu m$), $\tau_L' = 70$(corresponding to laser pulse duration of $200fs$); initial position of pulse peak $z_L' = 0$; initial electron position $x_i' = 0$, $y_i' = 0$, and $z_i' = 0$; initial phase $\phi_0 = 0$, normalized initial momentum of electron $p_0' = 1$, and $b_0 = 0.05$ (corresponding to a magnetic field of $5.34MG$), $b_0 = 0.1$ (corresponding to a magnetic field of $10.7MG$).

Figure 9.2 represents the variation of electron energy gain with respect to normalized propagation distance ξ. This gain has been examined for distinct values of laser spot size r_0' with intensity parameters $a_0 = 5$, 25, and 50. Higher energy gain appears with higher intensity for same spot size. Fig. 9.2(a) depicts energy gain of about $300MeV$ with $a_0 = 50$ and $r_0' = 150$. Feng *et al.* [49] reported that the beam waist is a key parameter for achieving the accelerating distance of the order of Rayleigh length with a focused Gaussian beams. From figures 9.2(b) and 9.2(c), one can observe the acceleration distance of about six times the Rayleigh length with $r_0' = 300$ and three times the Rayleigh length with $r_0' = 450$ respectively. We have plotted the variation of laser beam width parameter $f(z)$ with respect to an increasing value of normalized propagation distance and observe an increase in beam width parameter with the distance of propagation of laser pulse in plasma. Smaller the beam width stronger the laser field and vice versa. Hence, high acceleration is observed with a small beam width parameter. Thus it is the laser beam width parameter which is controlling the electron acceleration distance. We observe the acceleration and deceleration of electron while interaction with a Gaussian laser pulse in plasma, which is due to the asymmetry in intensity of CP Gaussian laser beam. This

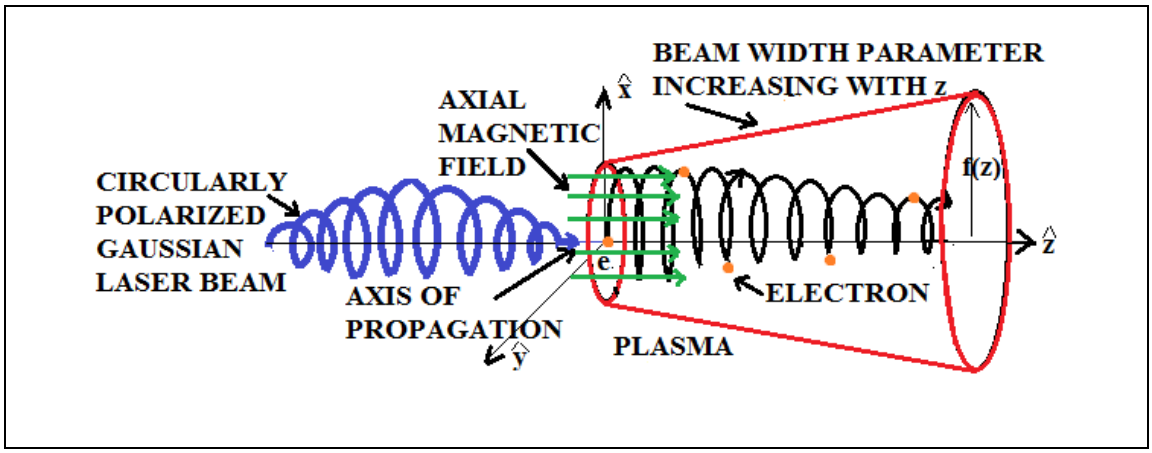

Figure 9.1. Schematic diagram for the acceleration of electron by a CP Gaussian laser pulse in plasma under the influence of axial magnetic field.

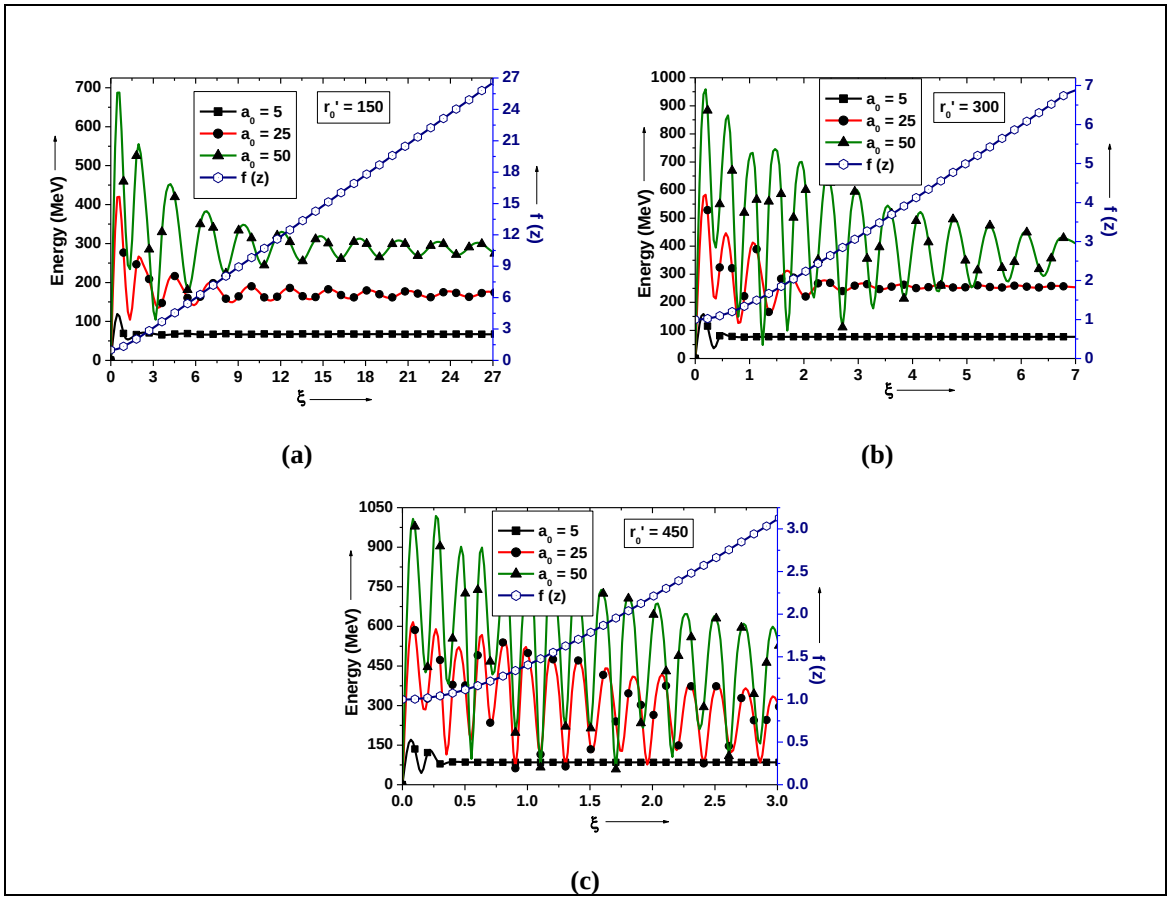

Figure. 9.2. Variation plot for electron energy gain with normalized distance and beam width parameter for the distinct values of laser spot size and intensity parameters. The other parameters are $\tau_L' = 70$, $\phi_0 = 0$, $p_0' = 1$, $z_L' = 0$, $x_i' = 0$, $y_i' = 0$, and $z_i' = 0$.

enforces the trapping and acceleration of electron for longer distance. The electron first gain high energy during interaction with the leading part of pulse. The gain saturates till reaching to the trailing part of pulse. The electron accelerating distance is calculated to be about three times the Rayleigh length with a LP chirped laser pulse of a large spot size $r_0' = 900$ in vacuum [122]. We observe the acceleration distance with a CP laser pulse is about three times the Rayleigh length for a smaller spot size $r_0' = 450$ in plasma. It is the betatron resonance which set up between accelerating electron and laser pulse during laser electron interaction in plasma. Figure 9.2(c) present the electron energy gain with a large beam spot size. In such case the wider acceleration and deceleration appears. The electron is accelerated where laser field is high in the vicinity of sharp focus and decelerates where field is weak. This makes an effective acceleration of electron in plasma.

Figure 9.3 represents the variation plot for electron energy gain as a function of normalized magnetic field b_0. This gain has been examined for different values of intensity parameter $a_0 = 5,\ 25,$ and 50 at different spot size $r_0 = 150,\ 300,$ and 450. The higher electron energy gain has been observed with magnetized plasma than that without magnetic field. We depict that the electron energy gain is responsive to the externally applied axial magnetic field. From fig. 9.3(a) one can find the optimum values of b_0 for higher energy gain with $a_0 = 5,\ 25,$ and 50 at $r_0 = 150$ as $0.12,\ 0.113$ and 0.125 respectively. Thus the optimum values of axial magnetic field remains small for high energy gain using high intensity laser pulse. One may notice that even for a small change in axial magnetic field, a significant change in electron energy appears. From fig. 9.3(b) and 9.3(c) the optimum values for high electron energy gain of the order of GeV with $r_0 = 300$ and 450 are appearing with normalized magnetic field value $b_0 \leq 0.17$. This corresponds to magnetic field of about $18.2MG$. Such value of magnetic field is experimentally feasible [113, 115].

Figure 9.4 represents the variation plots for electron energy gain as a function of ξ for $r_0' = 150$ and different intensity parameters. The variation with and without magnetic field has been plotted graphically for different intensity parameters $a_0 = 5,\ 25,$ and 50.

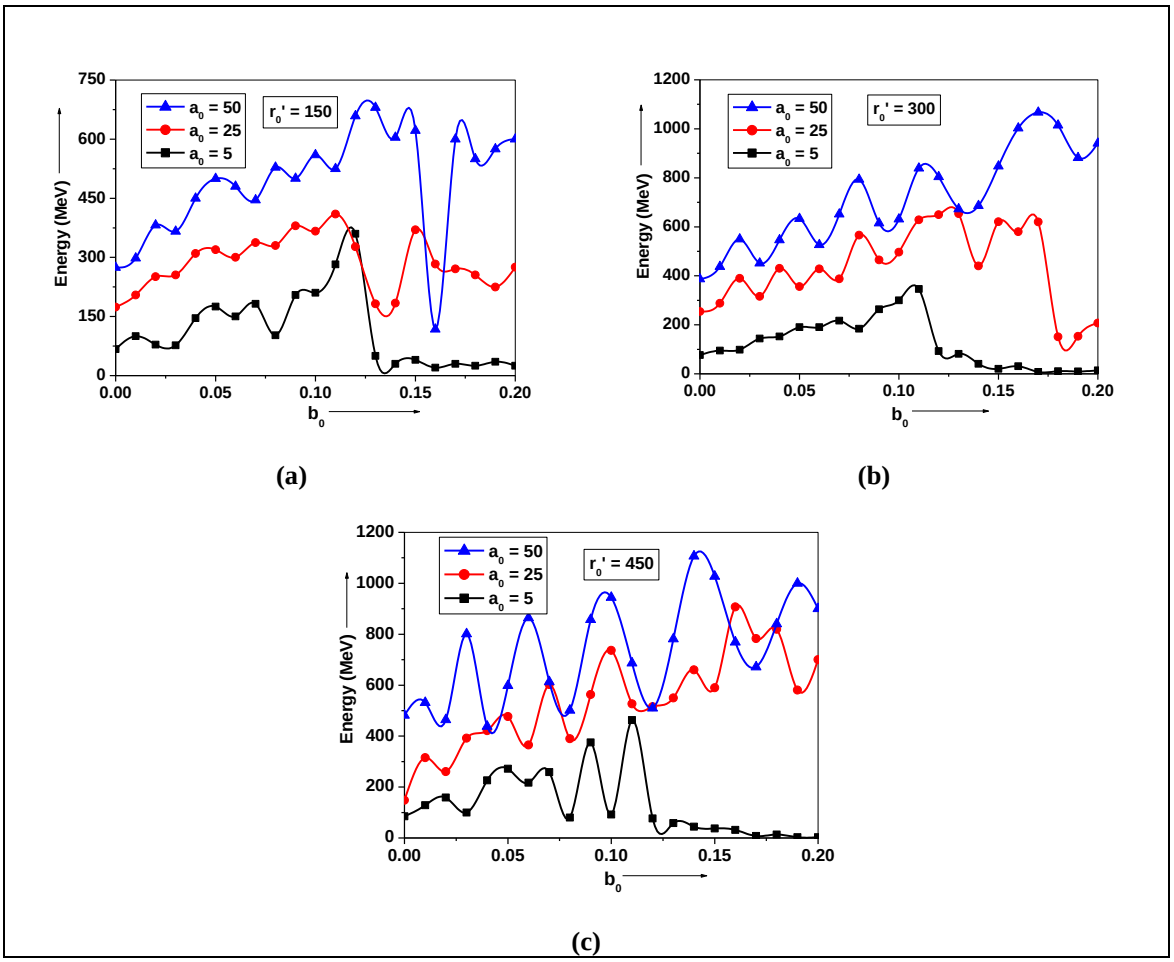

Figure 9.3. Variation plot for electron energy gain with normalized axial magnetic field b_0 for distinct values of laser spot size r_0' and intensity parameters $a_0 = 5$, 25, and 50. (a) $r_0' = 150$, (b) $r_0' = 300$, and (c) $r_0' = 450$. Rest of the parameters are as referred in fig. 9.2.

The magnetic field increases the strength of force component due to $\vec{v} \times \vec{B}$ experience by the electron, and hence maximizes the electron acceleration. After reaching to the maximum energy gain, it decelerates slightly due to weakening of field with increasing beam width parameter. It is the presence of applied axial magnetic field which supports the retaining of high energy for larger propagation distance. The electron energy gain then saturates. It is due to the betatron oscillations which set up between the electron and the electric field of the laser pulse. The electron retains high energy even in the weak field due to laser. One can observe from fig. 9.4(a), (b), and (c), that the accelerated electron

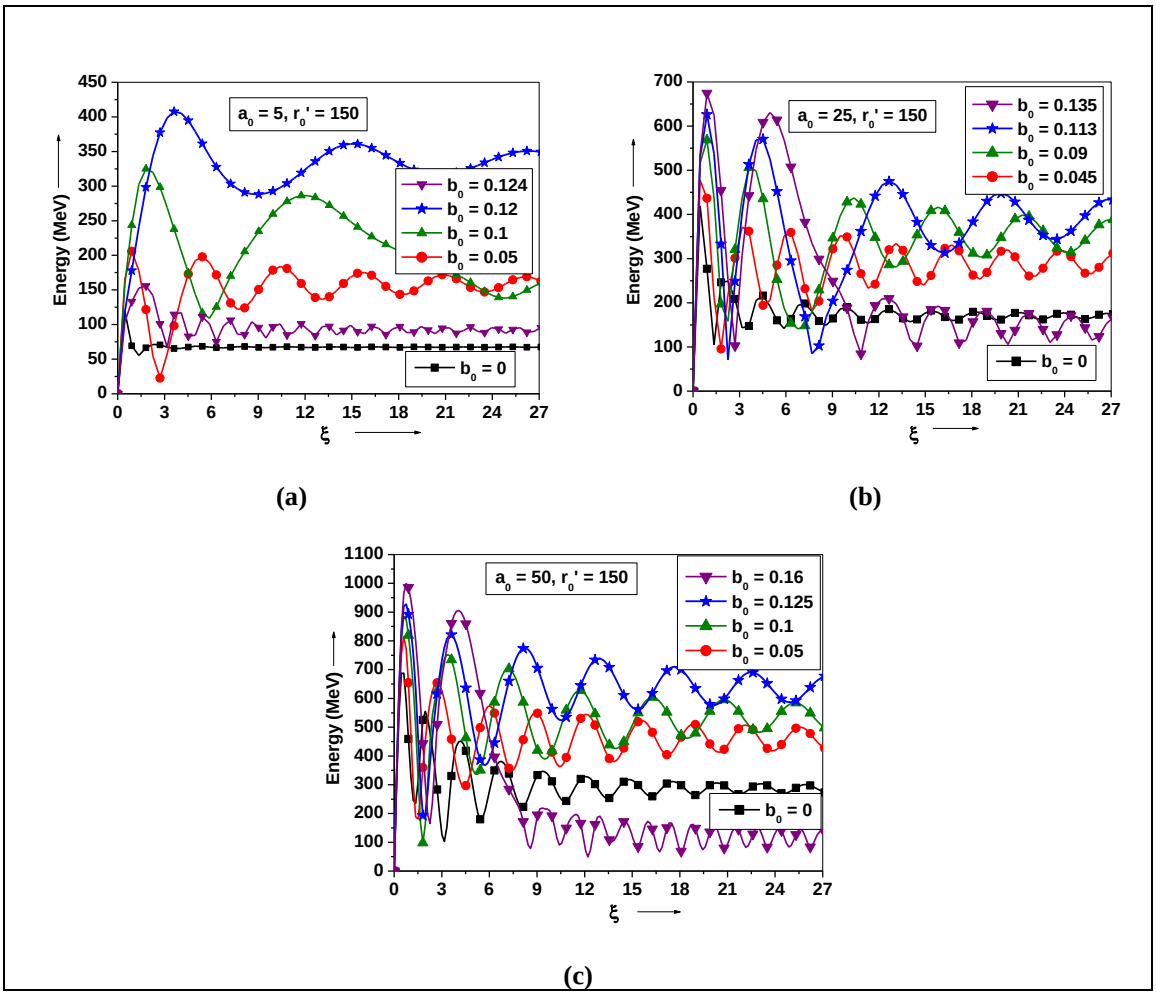

Figure 9.4. Variation plots for electron energy gain with normalized propagation distance ξ for distinct values of normalized magnetic field with laser spot size $r_0'=150$ and intensity parameters: (a) $a_0=5$, (b) $a_0=25$, and (c) $a_0=50$. Rest of the parameters are as referred in fig. 9.2.

retains high energy for larger distance. In the absence of magnetic field the electron gains and retains relatively lower energy than that in the presence of optimized field. Thus the electron energy gain is sensitive to the magnetic field. A small change in magnetic field significantly changes the electron energy gain. The optimum values of axial magnetic field b_0 for different intensity parameters a_0 are derived from fig. 9.3(a) for $r_0'=150$.

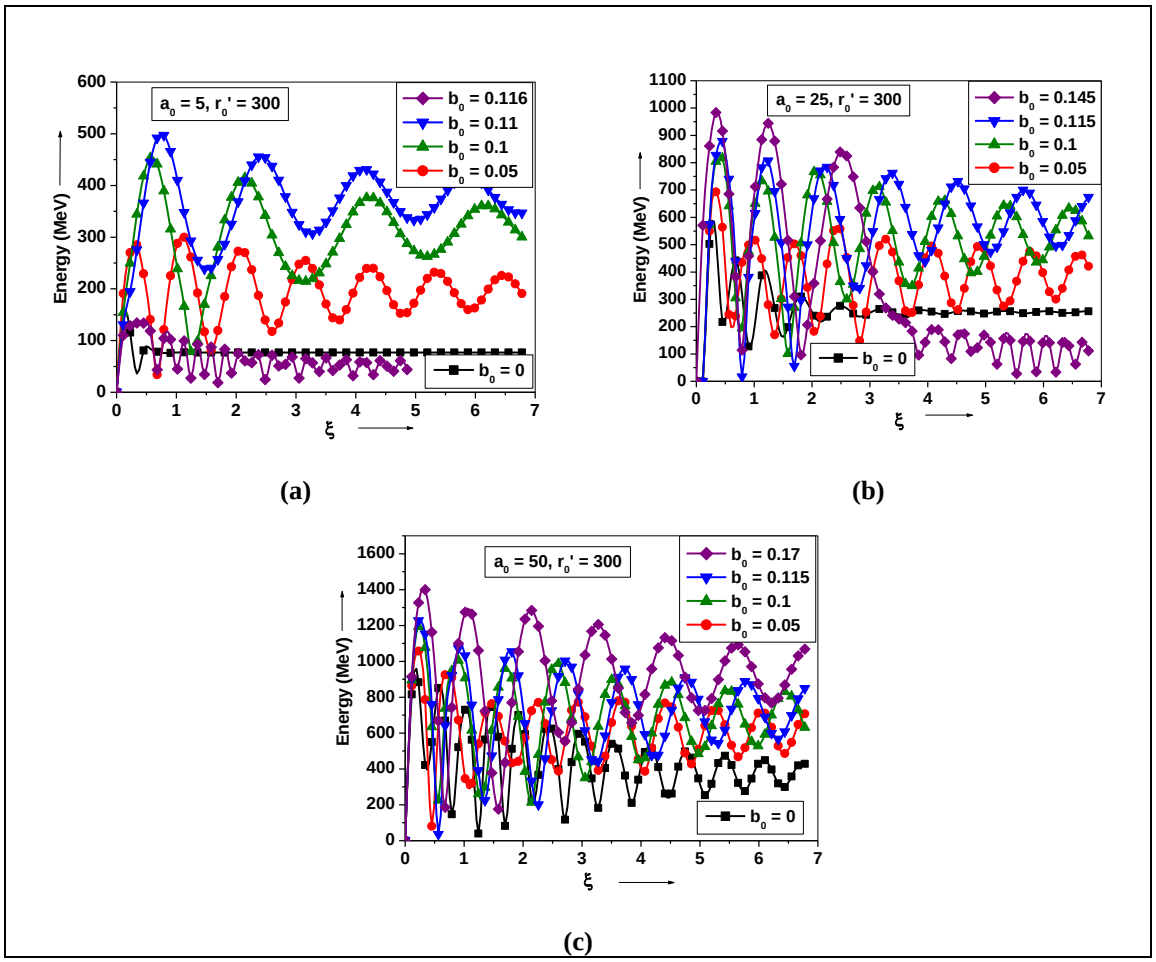

Figure 9.5. Variation plot for electron energy gain with normalized propagation distance ξ for distinct values of normalized magnetic field b_0 and intensity parameters with laser spot size as: (a) $a_0 = 5$, $r_0' = 300$ (b) $a_0 = 25$, $r_0' = 300$ (c) $a_0 = 50$, $r_0' = 300$. Rest of the parameters are as referred in fig. 9.2.

Figure 9.5 and 9.6 represents the variation plots for electron energy gain with respect to the normalized propagation distance ξ. In fig. 9.5(a) and 9.6(a), we see the variation for two different values of laser spot size $r_0' = 300$ and 450 with optimum values of axial magnetic field for $a_0 = 5$. The electron energy gain first increases while interaction with laser pulse. After attaining the maximum value, the electron decelerated due to increasing beam width and then energy gain saturates for larger distances.

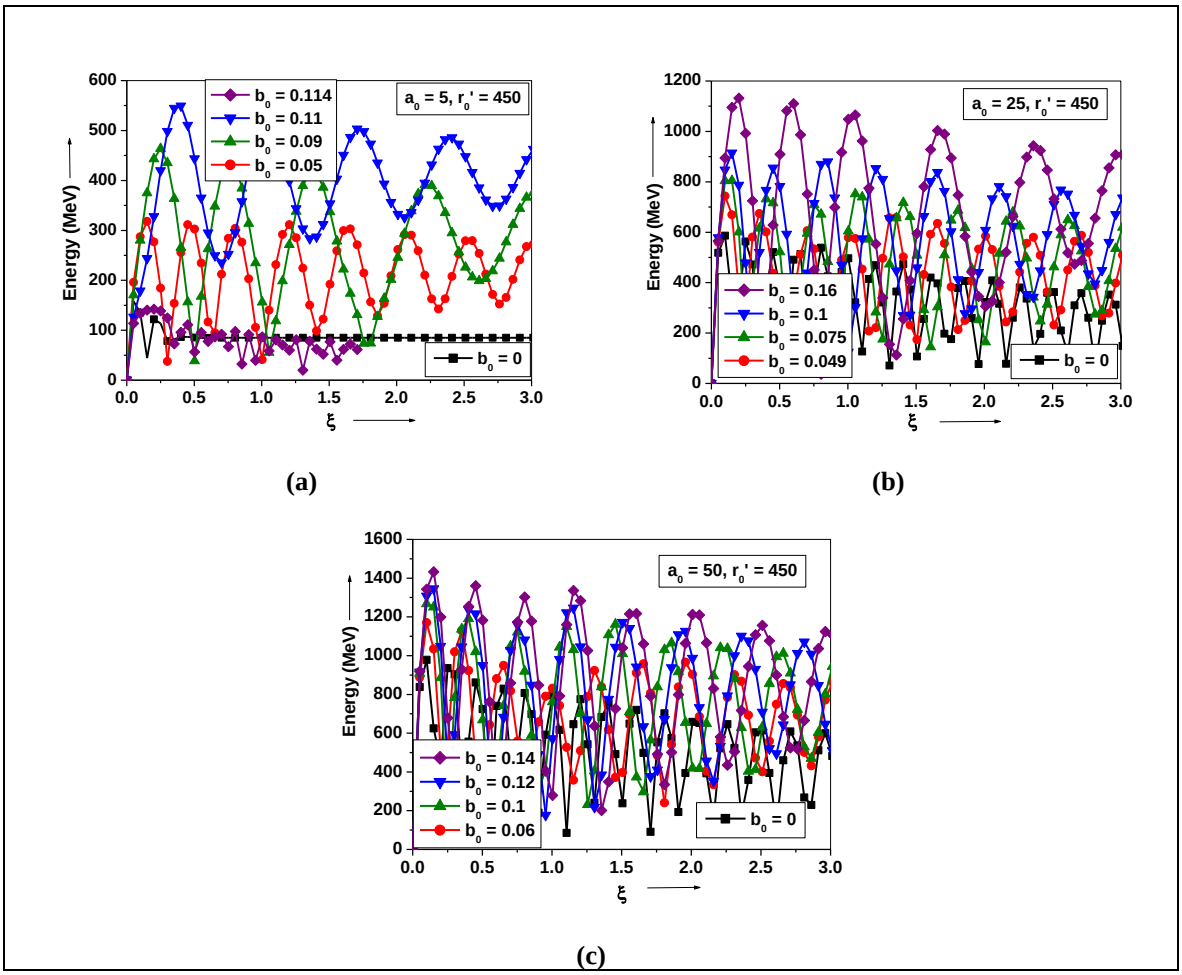

Figure 9.6. Variation plot for electron energy gain with normalized propagation distance ξ for distinct values of normalized magnetic field b_0 and intensity parameters with laser spot size as: (a) $a_0 = 5,\ r_0' = 450$ (b) $a_0 = 25,\ r_0' = 450$ and (c) $a_0 = 50,\ r_0' = 450$. Rest of the parameters are as referred in fig. 9.2.

Fig. 9.5(b) and 9.6(b) represents the variation of electron energy gain with ξ obtain with the optimum values of magnetic field b_0 with $a_0 = 25$ for $r_0' = 300$ and 450. With the optimum value of axial magnetic field and spot size, the electron gain higher energy with propagation distance due to resonance. As appearing an energy gain of $1GeV$ is achieved with laser intensity $a_0 = 50$ (corresponding to $I \sim 6.8\times10^{21}\ W/cm^2$) and spot size $r_0' = 300$ in the presence of axial magnetic field $b_0 = 0.115$ (corresponding to

12.3MG). The electron energy gain greater than $1GeV$ is achieved with same intensity, larger spot size $r_0' = 450$ and axial magnetic field $b_0 = 0.14$. We have calculated that the accelerating distance of electron is about three times the Rayleigh length. The same is depicted from figures 9.6. The higher energy gain is attained with higher values of laser intensities, optimum values of magnetic field, and laser spot size. The optimum value of magnetic field for a high energy gain is also sensitive with laser spot size. Thus it is the combined effect of laser spot size and magnetic field which attributes to high energy gain by accelerated electrons in magnetized plasma. Magnetic field is optimized with respect to laser spot size and intensity parameter.

Figure 9.7 represents the plots for the variation of electron acceleration gradient with accelerating distance z. The electron acceleration gradient [121] can be expressed with relation $d\gamma / dz = -e\vec{\beta}.\vec{E} / \beta_z$. The variation is plotted with propagation distance z for a CP Gaussian laser pulse for distinct values of intensity parameter $a_0 = 5$, 25, and 50 with laser spot size $r_0' = 150$, and $r_0' = 300$ and an optimum magnetic field b_0 as derived from fig. 9.3. An acceleration gradient of $59GeV / m$ was reported with a chirped femtosecond laser pulse of intensity of the order of $10^{19} W / cm^2$ for electron acceleration in vacuum [96]. Here we have observed about about $200GeV / m$ acceleration gradient with laser intensity $I \sim 6.92 \times 10^{19}\ W / cm^2$ in magnetized plasma. Higher electron acceleration gradient is obtained with higher values of laser intensity.

Figure 9.8 represents the plot for angle of ejection of electron with normalized propagation distance. The emittance of electron remains small even with higher intensity laser pulses. The angle θ of emittance and the final momentum of emitted electron is related as, $\tan\theta = (p_x^2 + p_y^2)^{1/2} / p_z$. Using Lorentz force factor, the emittance of electrons with z-axis can be written as, $\theta = \tan^{-1}(\sqrt{((\gamma^2 - 1) / \gamma^2 \beta_z^2) - 1}$. For energy gain of $450MeV$ with $a_0 = 50$ the angle of emittance is about 0.4° with $r_0 = 150$ and $b_0 = 0.05$.

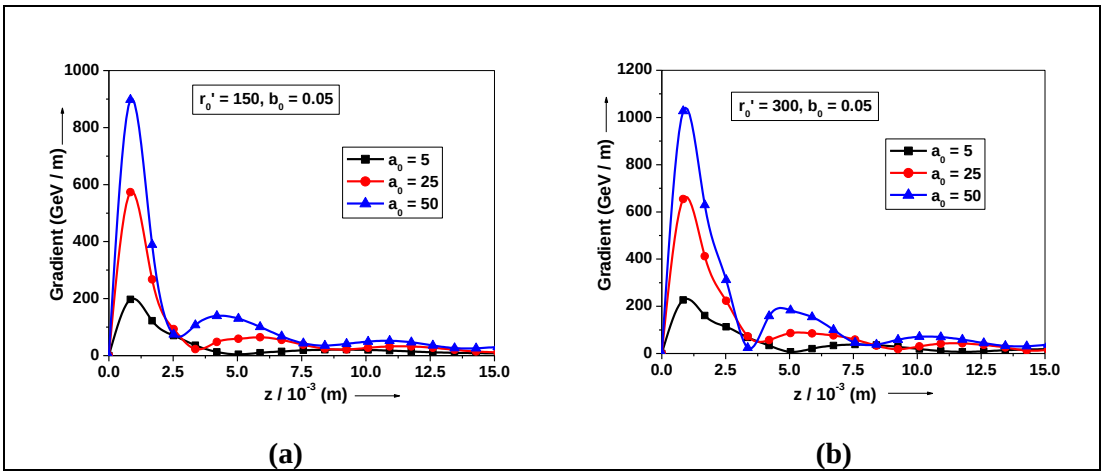

Figure 9.7. Variation plot for acceleration gradient with propagation distance z, for different intensity parameters $a_0 = 5$, 25, and 50 in the presence of normalized magnetic field $b_0 = 0.05$ with laser spot size: (a) $r_0' = 150$, and (b) $r_0' = 300$. Rest of the parameters are as referred in fig. 9.2.

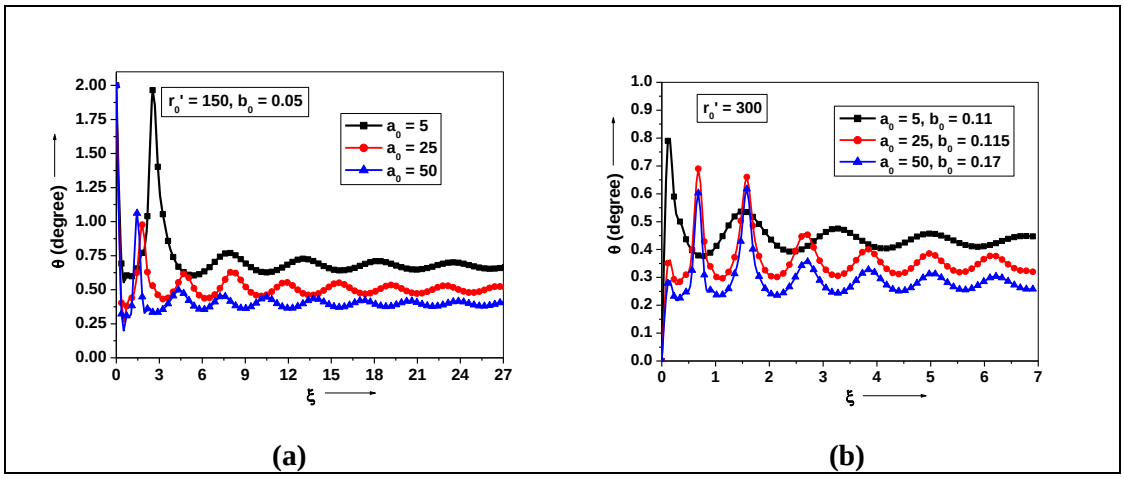

Figure 9.8. Variation plot for electron ejection angle with normalized propagation distance ξ for (a) $r_0' = 150$ at $a_0 = 5$, 25, and 50 with $b_0 = 0.05$ (b) $r_0' = 300$ at $a_0 = 5$, 25, and 50 with $b_0 = 0.11$, 0.115, and 0.17 respectively. Rest of the parameters are as referred in fig. 9.2.

On comparing fig. 9.8(a) and (b) we find that for a larger value of spot size and with optimum value of magnetic field the emittance appears relatively smaller than that with small value spot size. For an energy gain of $1GeV$ with $a_0 = 50$ the angle of emittance is 0.22° with $r_0 = 300$ and normalized magnetic field $b_0 = 0.17$. Thus the calculated values of angle of emittance of electron for higher energy gain remain small.

9.5 CONCLUSION

In this study we have highlighted the importance of beam width parameter of a CP Gaussian laser beam as well as the external axial magnetic field in obtaining a high electron energy gain in plasma. We have noticed an enhanced electron energy gain above $1GeV$ for laser intensity $a_0 = 50$ (corresponding to $I \sim 6.8\times10^{21}\ W/cm^2$) with laser spot size $r_0' = 450\ (\sim 75\mu m)$ under the influence of axial magnetic field $b_0 = 0.14$ (corresponding to $15MG$). We have also observed the sensitiveness of axial magnetic field on the electron energy gain. With an appropriate selection of laser beam spot size, a significant enhancement in electron energy gain with a relatively smaller scattering and higher acceleration gradient appears with axial magnetic field of optimum values. Thus, a rest electron in magnetized plasma can be accelerated to the order of GeV energy by selection of optimized value for laser spot size and axial magnetic field.